Atomic-based stabilization for laser-pumped atomic clocks

V. Gerginov, V. Shah, S. Knappe, L. Hollberg, and J. Kitching

Time and Frequency Division, National Institute of Standards and Technology, 325 Broadway Street M.S. 847, Boulder, Colorado 80305

Received February 6, 2006; revised March 17, 2006; accepted March 17, 2006; posted March 24, 2006 (Doc. ID 67843)

We describe a novel technique for stabilizing frequency shifts in laser-interrogated vapor-cell atomic clocks. The method suppresses frequency shifts due to changes in the laser frequency, intensity, and modulation index as well as atomic vapor density. The clock operating parameters are monitored by using the atoms themselves, rather than by using conventional schemes for laser frequency and cell temperature control. The experiment is realized using a chip-scale atomic clock. The novel atomic-based stabilization approach results in a simpler setup and improved long-term performance. © 2006 Optical Society of America

OCIS codes: 020.1670, 120.3930.

The application of precise timing in areas such as network communications and GPS navigation has motivated the development of compact, high-performance atomic frequency standards. Laser-interrogated vapor-cell frequency references are of special interest because of their reduced power dissipation and cost compared with lamp-operated devices. The requirements for small size have shifted the focus from conventional excitation methods based on microwave fields toward devices based on coherent population trapping[1,2] (CPT), for which no microwave cavities are required. The use of microelectromechanical systems provides an avenue for realizing the full potential for small CPT devices that simultaneously achieve much reduced power dissipation and can potentially be mass produced. Physics packages of chip-scale atomic clocks based on microelectromechanical systems with volumes of several cubic millimeters[3] and power consumption below 10 mW[4] have recently been demonstrated.

Most CPT-based atomic references are based on light from a diode laser modulated at microwave frequencies, which excites alkali atoms contained in a vapor cell. When the frequency difference between two components in the optical spectrum matches the frequency splitting of the atomic ground state, the optical fields pump some of the atoms in a superposition state that absorbs less power from the light fields. The decreased absorption is used to lock the local oscillator (LO) frequency to the atomic transition and stabilize it over long periods.

The frequency splitting of the atomic ground state can be shifted by both resonant and off-resonant[5] light fields through the ac Stark effect. To achieve good long-term frequency stability, it is therefore important to control the frequency and intensity of all participating light fields. The simplest stabilization scheme locks the laser frequency to an optical transition in the atoms by monitoring the light absorption and feeding the error signal back to the laser injection current. In addition, the temperature of the laser substrate is stabilized by using a thermistor temperature sensor and feedback to the laser substrate heater. In this Letter we propose and demonstrate a novel alternative to this conventional scheme where the actual parameters that determine the frequency of the clock—laser intensity, laser optical frequency, and modulation index—are all locked to a signal derived directly from the atomic spectroscopy. With this technique, the frequency shifts due to ac Stark shift can be reduced dramatically and the long-term frequency stability of the frequency reference improved. In addition, we propose to use the atomic absorption signal as a direct measure for the vapor temperature inside the cell.

The experimental measurements were performed with a CPT-based chip-scale atomic clock physics package similar to those described earlier.[3] A VCSEL die, emitting light at 795 nm, is mounted on a quartz substrate; a thin-film resistive heater deposited onto the substrate maintains the VCSEL temperature at around 80 °C. An external LO modulates the laser injection current at a frequency corresponding to half of the ground state hyperfine splitting of ^{87}Rb atoms (6.835 GHz). The divergent and linearly polarized laser beam passes through a neutral-density filter and a quarter-wave plate before entering a Rb vapor cell of 1 mm^3 internal volume.[6] The optical frequency of the laser carrier is tuned such that the first-order sidebands are in resonance with the two ground-state components and is locked by using modulation of the laser frequency at 17 kHz with 100 MHz depth. The optical frequency lock bandwidth was 30 Hz. The microfabricated vapor cell (its temperature maintained near 85 °C) is filled with a buffer gas mixture of argon and neon at total pressure of ~16 kPa, as well as isotopically enriched ^{87}Rb. The LO frequency is stabilized to the $m_F=0$ to $m_F=0$ ground-state CPT resonance. The CPT resonance linewidth is ~7 kHz with an absorption contrast of 3.3%.

Figure 1 highlights the differences between the conventional locking method [Fig. 1(a)] and the new methods proposed here. In the conventional scheme, the VCSEL and cell temperatures are stabilized by using thermistors mounted next to each component, and control feedback loops to the VCSEL heater and two indium-tin oxide thin-film heaters located on the cell windows, respectively. The laser frequency is locked to the maximum absorption of the first-order

0146-9592/06/121851-3/$15.00

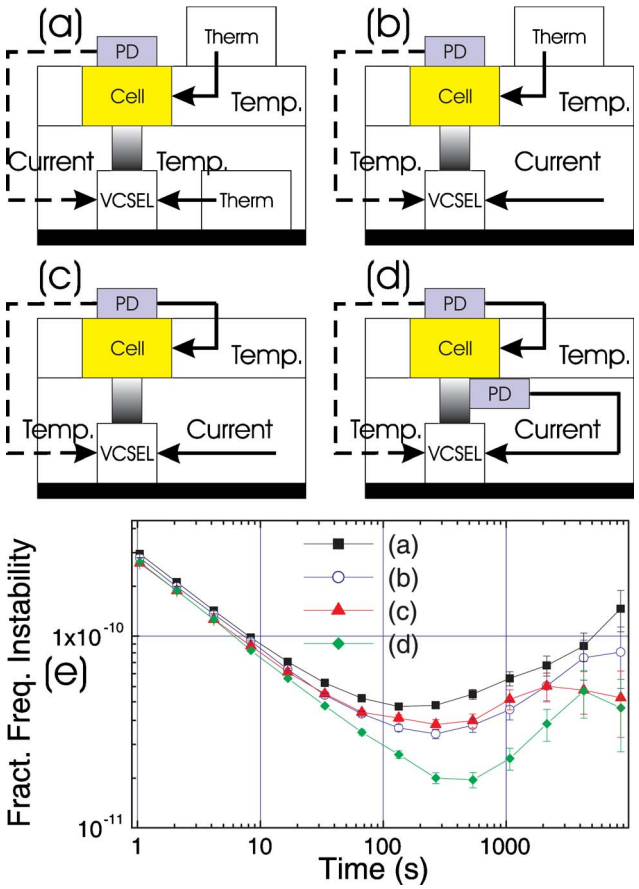

Fig. 1. (Color online) (a)–(d) Experimental setup for chip-scale atomic clock parameter control. Therm, thermistor; Temp., temperature control; Current, current control; PD, photodiode; VCSEL, vertical-cavity surface-emitting laser, solid lines, dc signals; dashed lines, phase detection signals. (a) Conventional setup. (b) Laser frequency is controlled by temperature feedback. (c) In addition to (b), cell temperature is controlled by atomic absorption. (d) In addition to (c), laser intensity is controlled by use of a photodetector. (e) Fractional frequency instability plots, corresponding to configurations (a)–(d).

sidebands by means of feedback to the laser injection current. The LO output power is chosen such that the first-order sideband amplitude is maximum. A plot of the fractional frequency instability for this conventional operating configuration is shown in Fig. 1(e) [trace (a), filled squares].

The first problem in the conventional stabilization scheme [Fig. 1(a)] results from varying temperature gradients between the laser active region and the thermistor. Under constant injection current, the temperature of the laser active region determines the laser optical frequency and power. A scheme shown in Fig. 1(b) and similar to the setup in Ref. 7 can be used to eliminate the temperature measurement of the laser substrate and stabilize the optical frequency of the laser. The laser is operated with a combination of a constant dc injection current and a superimposed ac modulation. The laser frequency is stabilized to the atomic resonance by feedback to the laser heater rather than the injection current. The bandwidth of the temperature control loop is limited to ~30 Hz by the thermal mass and conductivity of the laser baseplate. A plot of the fractional frequency instability under these conditions is shown in Fig. 1(e) [trace (b), open circles]. It can be seen that the reduced bandwidth of the servo loop does not degrade the short-term stability of the clock. This method of laser stabilization results in simpler setup, due to the elimination of the thermistor, and improved long-term clock performance.

A second problem with the conventional stabilization scheme [Fig. 1(a)] results from varying temperature gradients between the sensor measuring the cell temperature and the cell interior. Even though there are methods to reduce the collision-induced temperature dependence,[8,9] it still remains a source of frequency instability in clocks based on buffer gas high-pressure cells. However, the temperature of the cell walls also determines the alkali vapor density, and hence the optical absorption of the resonant light passing through the cell. Under typical operating conditions, the transmitted light power changes as a function of cell temperature (near a nominal temperature of 85 °C) by ~1%/K, a value similar to the change in the resistance of a typical thermistor (~4%/K). Figure 1(c) shows a control implementation that takes advantage of this temperature dependence. By feeding the dc signal from the photodetector behind the cell back to the cell heater, the cell absorption and therefore its relevant temperature is stabilized. The loop bandwidth was 0.2 Hz. A plot of the fractional frequency instability for this configuration is shown in Fig. 1(e) [trace (c), solid diamonds]. The improvement over the configuration of Fig. 1(b) is expected to be considerably more pronounced in a nonlaboratory environment, where the temperature can fluctuate significantly.

In all schemes described above, the laser power can still drift, either because the injection current of the laser drifts or because of aging of the laser die. These effects can be reduced by simultaneously stabilizing the optical frequency and total output power of the laser. To do this, a second photodetector is placed in front of the cell [Fig. 1(d)]. It collects a fraction of the expanding light beam. The laser output power can then be stabilized by feeding back to the laser current. A plot of the fractional frequency instability [improved by a factor of about two over the setup of Fig. 1(a)] in this configuration is shown in Fig. 1(e) [trace (d), solid diamonds]. At the same time, this technique simplifies the setup, because no thermistors are required, in contrast with previous work.[10,11] The stability of the laser and cell temperatures reaches 1 and 50 mK, respectively, limited by the optical frequency lock and the voltage references used to stabilize the photodetector dc levels.

In the experiments described above, a synthesizer with a very stable output power was used to modulate the VCSEL injection current. In portable CPT atomic clocks, the synthesizer is replaced with a compact low-power LO.[12] Changes in the output power of the LO or in the impedance of the VCSEL redistribute the optical power among the modulation sidebands. This, in turn, can change the clock frequency because of the ac Stark shifts from the resonant and

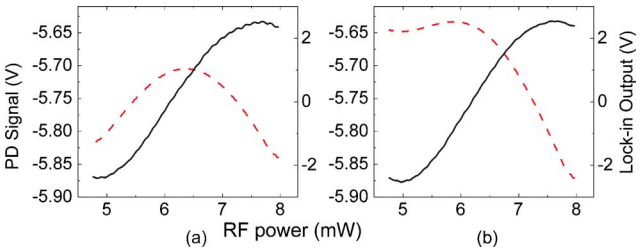

Fig. 2. (Color online) Photodetector output (dashed curve, left axis) and error signal (solid curve, right axis) as a function of RF power coupled to the laser. (a) Laser temperature stabilized using atomic absorption. (b) Laser temperature stabilized using a thermistor. The synthesizer was AM modulated at 1 kHz with 3% depth. The time constant of the lock-in amplifier was 10 ms and its sensitivity 1 mV.

off-resonant sidebands. Passive methods for minimizing clock frequency shifts due to changes in the light field of the laser are described in Refs. 5 and 13–15. In the passive methods, the clock frequency is made insensitive to changes in laser intensity by choosing the rf modulation index such that the ac Stark shifts of each individual spectral component compensate each other. These stabilization techniques are effective only if the modulation index of the laser or the LO power does not change.

We can carry out active stabilization of the sideband spectrum by modulating the rf power entering the laser and phase-sensitively demodulating the photodetector signal. Under optimal stabilization conditions [corresponding to Fig. 1(d)] a dispersive error signal is generated that passes through zero when the rf power is such that the optical power in the two first-order modulation sidebands is a maximum. The transmitted power and corresponding error signal are shown as a function of the rf power in Fig. 2(a). In this case, the amplitude of the CPT signal will also be optimized because the first-order sidebands, which generate the signal, now contain the maximum fraction of the total laser power.

Figure 2 clearly confirms that the stabilization architecture shown in Fig. 1(d) does in fact control the laser active region temperature, as opposed to the substrate temperature. Figure 2(b) shows the photodetector dc signal as the rf power is changed under the conventional locking scheme [Fig. 1(a)]. In addition to the roughly quadratic dependence generated by the change in the sideband spectrum, a linear dependence is also present. This linear drift is a result of the heating of the laser active region as the rf power increases. As the active temperature increases, the laser optical frequency would shift, but the laser frequency servo adjusts the laser current to compensate. The changing laser current alters the laser intensity and causes the increase in the photodetector signal observed in Fig. 2(b). By contrast, no linear dependence is observed in Fig. 2(a), when the atomic-based locking architecture is implemented. This measurement indicates that the laser active-region temperature is considerably more stable under conditions when the rf power is changing, and therefore independently confirms that the locking architecture in Fig. 1(d) is functioning as anticipated.

In conclusion, a new method is realized for atomic-based stabilization of laser-pumped atomic clocks. The method is based on direct measurement of parameters important for the performance of an atomic-frequency reference using the atoms themselves and allows simultaneous stabilization of the laser optical frequency, output power, and microwave modulation index as well as temperature of the vapor cell.

This work was supported by the Microsystems Technology Office of the U.S. Defense Advanced Research Projects Agency (DARPA). This work is a contribution of the National Institute of Standards and Technology, an agency of the U.S. government. V. Gerginov is also with the Department of Physics, University of Notre Dame, Notre Dame, Indiana 46556. V. Shah is also with the Department of Physics, University of Colorado, Boulder, Colorado 80309. V. Gerginov's e-mail address is vgergino@nd.edu.

References

1. E. Arimondo, Prog. Opt. **35**, 257 (1996).
2. J. Vanier, Appl. Phys. B **81**, 421 (2005).
3. S. Knappe, L. Liew, V. Shah., P. D. D. Schwindt, J. Moreland, L. Hollberg, and J. Kitching, Appl. Phys. Lett. **85**, 1460 (2004).
4. R. Lutwak, J. Deng, W. Riley, M. Varghese, J. Leblanc, G. Tepolt, M. Mescher, D. K. Serkland, K. M. Geib, and G. M. Peake, in *Proceedings of the Annual Precise Time and Time Interval (PTTI) Systems and Applications Meeting* (36th) (U.S. Naval Observatory, 2004) (CD-ROM).
5. M. Zhu and L. Cutler, in *Proceedings of the Annual Precise Time and Time Interval (PTTI) Systems and Applications Meeting* (32nd) (U.S. Naval Observatory, 2000) (CD-ROM), pp. 311–324.
6. L. A. Liew, S. Knappe, J. Moreland, H. Robinson, L. Hollberg, and J. Kitching, Appl. Phys. Lett. **84**, 2694 (2004).
7. T. Okoshi and K. Kikuchi, Electron. Lett. **16**, 179 (1980).
8. W. Happer, Rev. Mod. Phys. **44**, 169 (1972).
9. J. Vanier and C. Audoin, *The Quantum Physics of Atomic Frequency Standards*, 1st ed. (Adam Hilger, 1989).
10. S. Yamaguchi and M. Suzuki, IEEE J. Quantum Electron. **19**, 1514 (1983).
11. D. E. Janssen and M. W. Levine, U.S. Patent 6,222,424 (April 24, 2001).
12. A. S. Brannon, J. Breitbarth, and Z. Popovic, in *2005 IEEE MTT-S Symposium Digest* (IEEE, 2005), p. 1535.
13. J. Vanier, A. Godone, and F. Levi, in *Proceedings of the 1999 Joint Meeting of the European Frequency and Time Forum, 1999 and the IEEE International Frequency Control Symposium, 1999* (IEEE, 1999) pp. 96–99.
14. M. Zhu and S. Cutler, U.S. Patent 6,201,821 (March 13, 2001).
15. C. Affolderbach, C. Andreeva, S. Cartaleva, T. Karaulanov, G. Mileti, and D. Slavov, Appl. Phys. B **80**, 841 (2005).